The Interannual Variability and Trend of Precipitable Water over Southern Greece

P. A. Kassomenos

Laboratory of Meteorology, Department of Physics, University of Ioannina, Ioannina, Greece

G. R. McGregor

Department of Geography, King's College London, London, United Kingdom

(Manuscript received 25 January 2005, in final form 30 June 2005)

ABSTRACT

The precipitable water (PW) content was estimated over southern Greece for three atmospheric layers, using 28-yr twice-daily radiosonde measurements of temperature, humidity, and atmospheric pressure. Precipitable water demonstrates considerable variation at the monthly and interannual time scales as well as statistically significant upward trends at the annual level and for June–August (JJA) and September–November (SON). The relationship between PW and surface climate was also found to vary by season and surface climate variable. Disaggregation of seasonal PW trends by synoptic type revealed that seasonal trends might be attributed to increases in moisture in a limited number of airmass types such that maritime air masses appear to be becoming moister while their continental counterparts are drying. Despite fundamental changes to the intrinsic PW properties of air masses for some synoptic categories, the significance of these for determining the overall trend in seasonal PW levels is related to their weighted contribution as determined by changing airmass frequency. Consequently, the climatological effects of a moistening or drying air mass may be offset by a declining frequency. It is also shown that increasing PW trends cannot be attributed unequivocally to airmass warming as significant increases in PW have occurred in conjunction with falling temperatures in some seasons and airmass types. Accordingly, factors other than the commonly assumed global-warming-related increase in atmospheric moisture via the link between temperature and saturation vapor pressure must be considered if the mechanisms responsible for PW trends over southern Greece are to be fully understood.

1. Introduction

Atmospheric water vapor plays a significant role in the water and heat processes of the climate system. Fluxes of water vapor link the main components of the hydrological cycle and the release of energy into the atmosphere and, via the process of condensation in the upper atmosphere, provide a fundamental source of energy for driving global atmospheric circulation. Atmospheric water vapor is also critical for maintaining an equitable climate on earth, as it is responsible for a considerable proportion of the natural greenhouse gas effect (Bony and Duvel 1994; Bokoye et al. 2003; Forster and Shine 2002; Forster and Collins 2004; Marsden and Valero 2004; Otterman et al. 2002). Moreover, unlike other greenhouse gases, water vapor is highly variable over space and time, both horizontally and vertically. Despite water vapor's obvious importance for climate and life on earth, it has received less attention in the literature compared to the other greenhouse gases. Recently however, there has been heightened interest in water vapor, due not only to its radiative properties, but because trends in tropospheric water content may be an indication of global-warming-related changes in the nature of the hydrological cycle (Ohmura and Wild 2002; Trenberth 2004).

Although there have been developments in satellite-based measurements of water vapor (Gutman et al. 2004; Li et al. 2003; Sajith et al. 2003) investigations aimed at exploring for trends in tropospheric moisture have tended to rely on temperature and humidity measurements from radiosondes because of their compara-

Corresponding author address: Dr. Paulos Kassomenos, Laboratory of Meteorology, Dept. of Physics, University of Ioannina, P.O. Box 1186, 45110 Ioannina, Greece.
E-mail: pkassom@cc.uoi.gr

tively long record length (Ross and Elliott 2001). Such investigations have used radiosonde temperature and humidity measurements to derive a range of atmospheric moisture descriptors including mixing ratio and precipitable water (PW). Notwithstanding the measure used, or the technique employed for estimating atmospheric moisture, studies have revealed that tropospheric moisture not only displays a considerable deal of intraseasonal to interannual variability (Chen and Tzeng 1990; Chen et al. 1996a,b; Kane 1996; Elliott and Angell 1997; Simmonds et al. 1999; Liu and Stewart 2003; Long et al. 2000; Myers and Waliser 2003; Phillips and McGregor 2001; Simmonds et al. 1999; Smirnov and Moore 2001; Vladimir et al. 2002; Zveryaev and Chu 2003) but also in some cases strong trends (Angell et al. 1984; Gutzler 1992; Hense et al. 1988; Ross and Elliott 2001; Zhai and Eskridge 1997).

As most studies of tropospheric moisture trends have focused on regions other than southern Europe, where significant changes in hydroclimatological characteristics are predicted with climate change (McGregor et al. 2005; Parry 2000), the purpose of this paper is twofold: first, to establish the nature of the interannual variability in PW and whether statistically significant trends in PW exist over southern Greece and, second, to assess the degree to which any identified trends may be explained by an analysis of the interannual frequency of airmass types and trends in their intrinsic airmass moisture properties.

2. Data and methodology

In this study PW is used as an index of atmospheric water vapor. It is defined as the depth of water that would result if all the water vapor in a unit column of air between two pressure levels was condensed and precipitated to the ground (McGregor and Nieuwolt 1998).

Precipitable water between two pressure levels p_i and p_{i+1} was calculated by

$$\mathrm{PW} = -\frac{1}{g}\int_{p_i}^{p_{i+1}} q\,dp,$$

where q and dp are specific humidity and pressure difference, respectively (Peixoto and Ort 1992).

TABLE 1. Synoptic category characteristics by season (adapted from Kassomenos 2003a,b).

SC	Winter	Summer
1	Low pressure system located over Middle East is combined with an anticyclone located over the Iberian Peninsula. Weak northerly flow over the Aegean. High radiation and low humidity levels.	Weak pressure gradient over Greece, with establishment of local circulation. Low solar radiation and temperature and high humidity levels.
2	Low pressure system located over the northern Balkans; weak pressure gradient over Aegean. Weak westerly flow; highest solar radiation and high temperature levels.	Anticyclone over western and central Europe combines with a low over the Middle East causing strong N-NE winds over the Aegean. Highest solar radiation and air temperature levels.
3	An anticyclone is located over the Iberian Peninsula; weak pressure gradient over eastern Mediterranean. NE winds, low radiation and temperature, and extensive cloudiness.	Very weak pressure gradient over Aegean; intense local circulations. High humidity levels; low solar radiation.
4	Cyclonic activity over Iberian Peninsula, strong southerly flow, and warm advection over Greece. Low solar radiation; high daily maximum temperature levels.	Weak NE flow over Aegean due to the combination of an anticyclone over western Europe with a low over Middle East. Temperature and humidity levels are lower than those of class 2.
5	A deep low is located over the Netherlands and North Sea; strong pressure gradient and southerly flow over the Aegean. Low radiation and high humidity levels. Warmer and more humid than SC 4.	
6	An anticyclone located over eastern Europe causes strong pressure gradient over the Aegean. Strong NE winds; lowest values of temperature and humidity.	
7	A low is located over the central Mediterranean and southern Italy. Pressure gradient over the Aegean is weak. High humidity and temperature levels, extensive cloudiness, precipitation, and weak southerly flow.	
8	Low pressure system is located south of Crete combined with an anticyclone located over eastern Europe that produces a strong pressure gradient over the Aegean with intense northerly flow. Low solar radiation and low daily maximum temperature and humidity levels.	

The requisite data for calculation of PW were extracted from twice-daily radiosonde soundings and surface observations of temperature, relative humidity, and barometric pressure at 0000 and 1200 UTC for World Meteorological Organization (WMO) station 16716 of the Greek Meteorological Service located at the Hellinicon Airport, Athens, for the period 1974–2001. Although other upper-air stations exist for Greece (Thessolaniki and Heraklion) the short duration and incompleteness of their records precluded them from inclusion in this analysis.

A major concern for any climatological analysis is the issue of data homogeneity (Peterson et al. 1998). This is especially true in the case of using radiosonde data for establishing trends in atmospheric moisture (Elliott and Gaffen 1991; Free et al. 2002, 2004; Gaffen et al. 2000; Lanzante 1996, 2003a,b; Zhai and Eskridge 1996; Zveryaev and Chu 2003). Homogeneity was tested for using the Jonckheere–Terpstra (JT) homogeneity test, which is a distribution-free test that assesses whether k independent samples are from the same population. It is appropriate for testing whether there are step changes in data that are either continuous or ordered by category or time. The JT test is considered to be more powerful than the Kruskal–Wallis test (Hollander and Wolfe 1973), which is commonly applied in homogeneity testing (Peterson et al. 1998). Application of the JT test revealed that all radiosonde and surface temperature and humidity data at 0000 and 1200 UTC were homogenous. Further, the amount of missing data was limited ranging between 93% and 99%.

Since the radiosonde data were available at 50-hPa intervals (1000, 950, 900, 850, 800, 750, 700, 650, 600, 550, 500 hPa) we calculated the PW in the layers between the surface and the corresponding isobaric layer. Initially the maximum and minimum values of PW were estimated and then daily values were used to calculate monthly, seasonal [December–February (DJF), March–May (MAM), July–August (JJA), September–November (SON)], and annual values of the mean and standard deviation. To understand the distribution of PW by month, PW values were binned into 12 categories for each isobaric layer. Precipitable water was calculated for 0000 and 1200 UTC separately. For reasons of simplicity we have chosen to present results for the following layers: surface–850 hPa, surface–700 hPa, and surface–500 hPa (henceforth 850, 700, 500 hPa). Total PW refers to the PW between the surface and 500 hPa. Further, as PW at 1200 and 0000 UTC are highly correlated ($r^2 = 0.85$, significant at the 0.01 level) PW values at 1200 UTC are focused upon. Because diurnal variations in PW have not been considered, the

Table 1. (*Continued*).

SC	Spring	Autumn
1	Deep low is located over Black Sea; strong pressure gradient over Aegean. High solar radiation and low temperature and humidity levels.	Low pressure system is located west of Italy; weak pressure gradient over Aegean Sea. Low radiation and high humidity levels.
2	An extended anticyclone is located over Europe and a low pressure system is positioned over Turkey; northerly flow over the Aegean. Lowest solar radiation, temperature, and humidity levels.	An extended anticyclone is located over Russia; strong pressure gradient over the Aegean. Low solar radiation, temperature, and humidity levels; NE winds.
3	An anticyclone is located over Russia with a strong pressure gradient over the Aegean. Strong NE winds; low solar radiation, humidity, and temperature levels.	An anticyclone is located over central Mediterranean; weak pressure gradient over Aegean. High values of solar radiation, temperature, and humidity.
4	An anticyclone is located over Europe; very weak pressure gradient over Aegean. Sea breezes and other local circulations. High solar radiation, temperature, diurnal temperature range, and humidity levels.	An anticyclone is located over Ukraine; strong pressure gradient over Aegean Sea. High temperature, solar radiation, and low humidity levels.
5	Low pressure system is located over Europe the pressure gradient over the Aegean is weak. Southerly flow, enhanced solar radiation, and diurnal temperature range and humidity levels.	Low pressure system is located over Italy and Greece; strong pressure gradient over Aegean Sea. Low solar radiation, temperature, and humidity levels, and strong NW winds.
6	A low pressure system is located over Italy; strong pressure gradient over the Aegean. Southerly strong winds, low values of solar radiation, and high humidity levels.	An anticyclone is located over the Iberian Peninsula; weak pressure gradient over the Aegean sea. Diurnal temperature range is high while temperature, humidity, and solar radiation are low.
7	Low pressure system is located over NW Africa. Pressure gradient over the Aegean is weak, causing local circulations. Humidity and solar radiation are high.	S-SE flow over Greece due to an extended low pressure system located over the central Mediterranean. Low solar radiation and high relative and absolute humidity levels
8	An anticyclone is located over the western Mediterranean; strong pressure gradient over Aegean. NW flow.	Strong northerly flow over the area. Lowest solar radiation, temperature, and humidity levels.

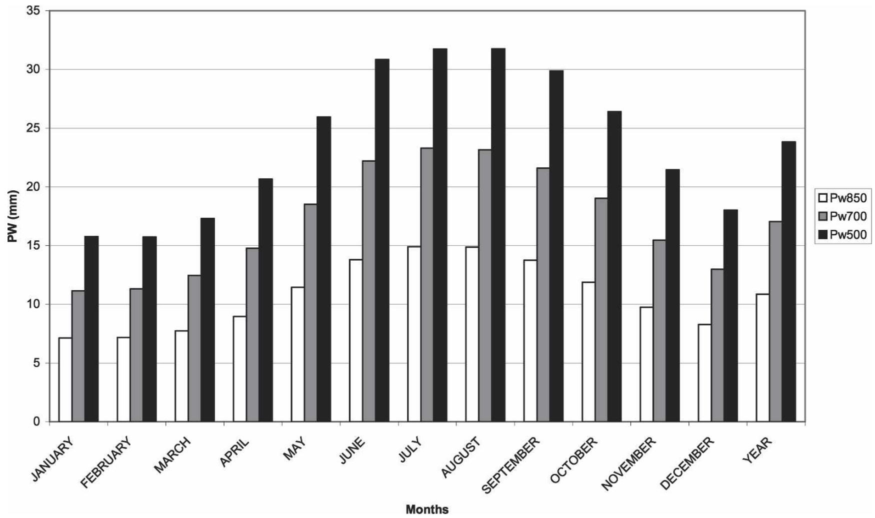

FIG. 1. Monthly distribution of total PW over southern Greece at 1200 UTC.

PW values for 1200 UTC should be treated as a proxy of total PW, which is acceptable for the purposes of this study as PW trends are the major concern, not the absolute values of PW. Linear regression analysis was used to test for trends in PW as in Ross and Elliott (2001).

So as to understand the possible synoptic origins of the interannual variation and seasonal trends in PW, days were stratified according to a computer-assisted seasonal categorization of synoptic types for southern Greece (Kassomenos 2003a,b). The synoptic types represent different combinations of the basic airmass properties of dry-bulb and dewpoint temperature, cloud cover, atmospheric pressure, wind speed, and wind direction. Daily values of PW were organized according to four synoptic categories for JJA and eight for DJF, SON, and MAM for each of the 28 years. Mean PW was then calculated for the days falling into each synoptic category (SC) by year and season. Subsequently the association between synoptic category frequency and seasonal PW was assessed as well as the trend in PW for each synoptic category by season. Details of the characteristics of the synoptic categories are presented in Table 1. In general, the synoptic categories represent situations typified by high or low pressure dominating Greece, the transition between centers of high and low

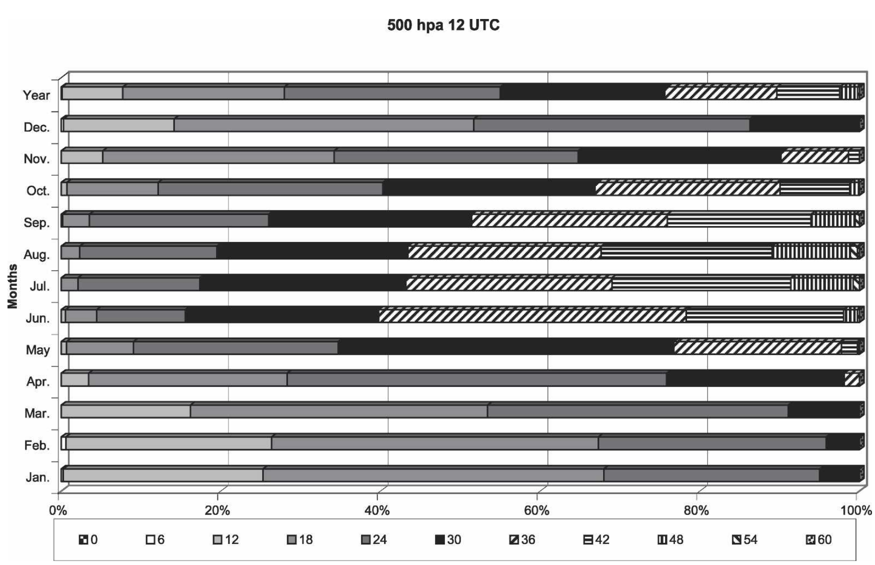

FIG. 2. Frequency distribution of total PW (surface to 500 hPa) at 1200 UTC.

TABLE 2. Correlation between surface climate and seasonal and annual precipitable water for three pressure levels, 850, 700, and 500 hPa, where *, **, and *** indicate significance at the 0.1, 0.05, and 0.01 levels, respectively.

Season	Climate variable	850PW	700PW	500PW
DJF	Temperature	−0.20	−0.21	−0.24
	Precipitation	0.31	0.34*	0.30
MAM	Temperature	−0.04	−0.11	−0.12
	Precipitation	−0.05	0.07	0.10
JJA	Temperature	0.34	0.31	0.26
	Precipitation	0.45**	0.38**	0.39**
SON	Temperature	−0.41**	−0.41**	−0.34*
	Precipitation	0.04	0.05	0.05
Annual	Temperature	0.05	0.03	0.04
	Precipitation	0.26	0.33	0.39**

pressure as would be found for strong zonal flows and associated frontal zones, or where the position of a center of low or high pressure produces a strong meridional flow over Greece from either the south or north. These general atmospheric pressure configurations influence whether maritime or continental air masses are advected over Athens and Greece as a whole. Consequently interannual variations and trends of the frequency of days belonging to each SC may have a marked impact on PW climates over Greece.

3. Results

a. Climatology and interannual variability

The monthly distribution of PW by isobaric layer is shown in Fig. 1 for 1200 UTC. On a monthly basis PW presents its maximum value during July and August when PW between the surface and 500 hPa reaches 30–32 mm. January and February possess the lowest PW amounts (Fig. 1). On an annual basis, 45.7% and 72.1% of the total PW is contained between the surface and 850- and 700-hPa levels, respectively. Although PW varies by season, the relative contribution by isobaric layer to total PW at 1200 UTC is quite constant across the four seasons. For example 72.5% and 71.6% of the total PW is contained between the surface and 700 hPa for JJA and DJF, respectively. Figure 2 presents the monthly frequency distribution of total PW by 12 categories. For January, February, and March, PW values between 15 and 18 mm dominate (in excess of 40% of the days), followed by values in the range of 18–24, 12–18, and 24–30 mm in decreasing order of importance. During the warm period from June to August, more than 30% of the days have PW values in excess of 30 mm. On a yearly basis more than 40% of the days possess PW values between 18 and 30 mm (Fig. 2). In relative terms similar frequency distributions are apparent for the surface to 850- and 700-hPa isobaric layers (not shown here) such that there is a shift to a higher frequency of high PW values in JJA and lower values in DJF.

TABLE 3. Precipitable water characteristics (mm) by synoptic category.

	Synoptic category							
	1	2	3	4	5	6	7	8
DJF	14.7	17.3	15.4	19.9	20.1	11.6	19.5	16.4
MAM	19.9	14.4	16.9	27.0	22.4	22.0	21.1	18.8
JJA	32.4	28.9	36.1	27.2				
SON	28.4	22.7	31.2	23.8	26.0	22.5	29.5	16.8

Of interest is the climatological association between

(a)

(b)

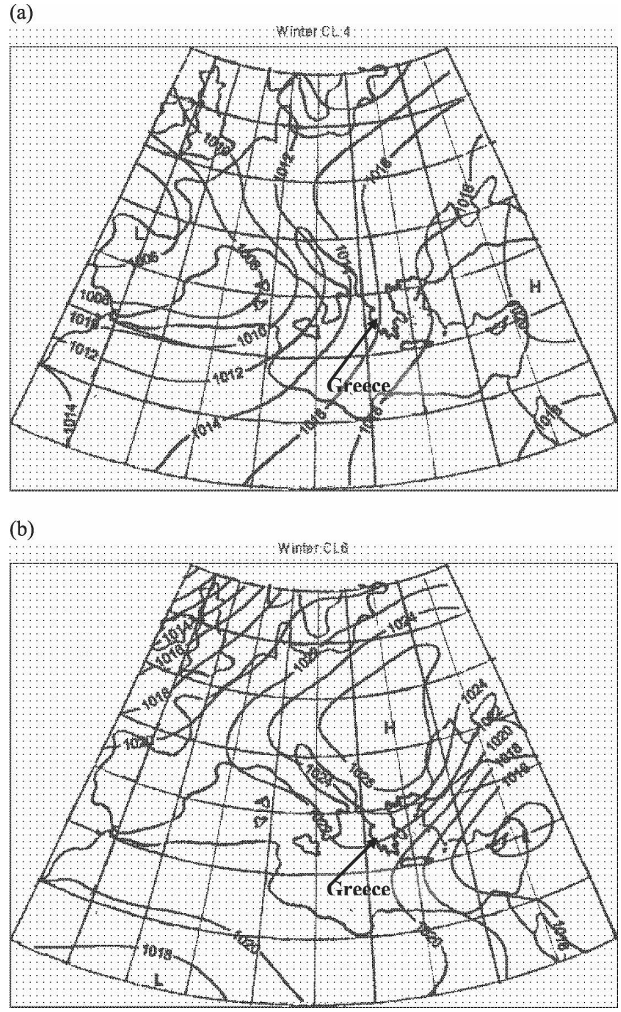

FIG. 3. Representative synoptic situations for DJF synoptic categories (a) 4 and (b) 6 associated with advection of contrasting air masses over Greece (from Kassomenos 2003a).

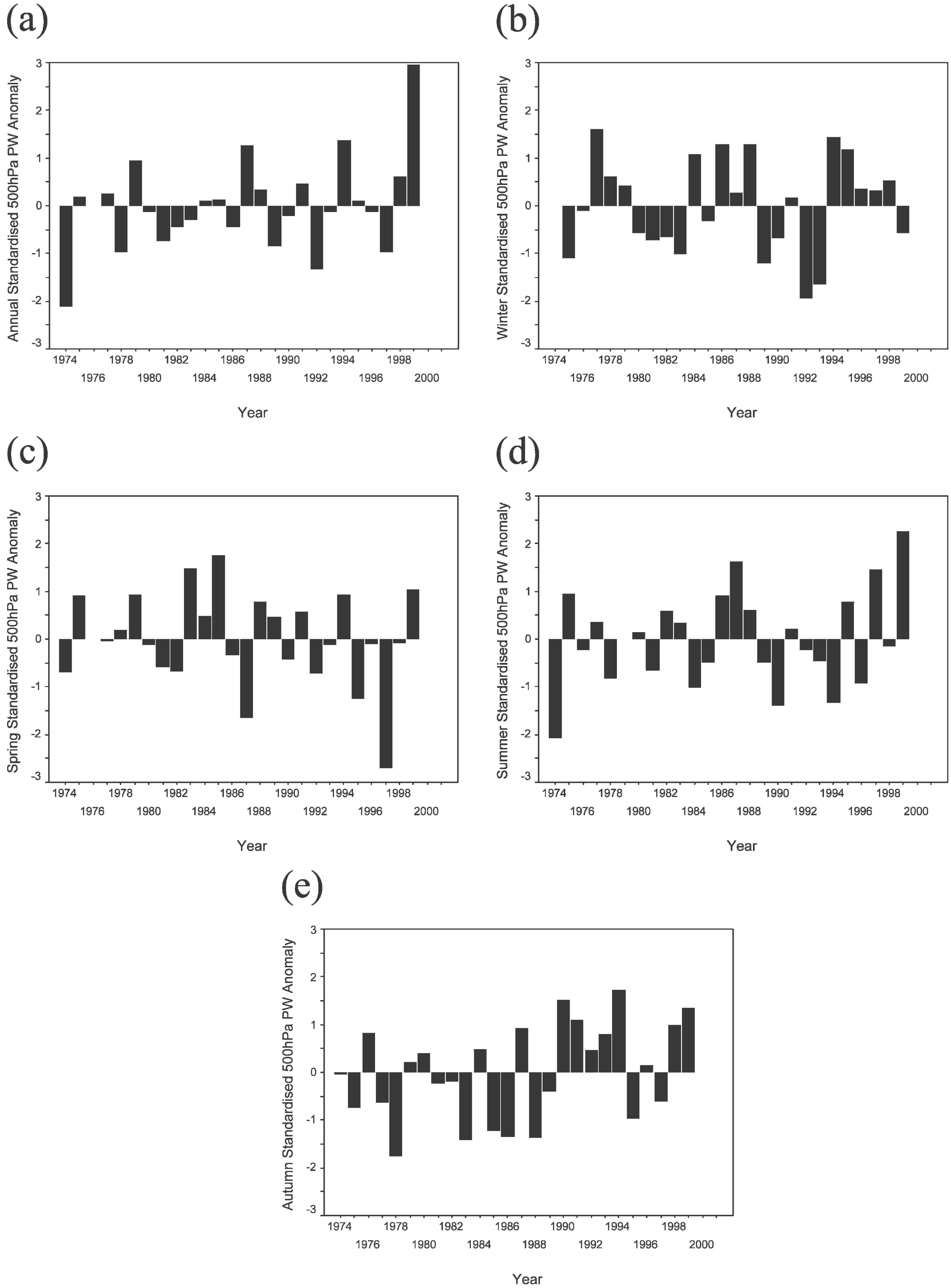

FIG. 4. Interannual variation of total PW (surface to 500 hPa): (a) annual, (b) DJF, (c) MAM, (d) JJA, and (e) SON.

PW and surface climate, as through influencing radiative transfer and setting a limit on the amount of moisture available for precipitation, atmospheric moisture may possess links with surface temperature and precipitation (Chrysoulakis and Cartalis 2002). On an annual basis mean surface temperature is not correlated with PW to any extent (Table 2). Consideration of the seasonal distribution, however, reveals near-significant (at the 0.1 level) positive associations between PW and temperature for JJA, but statistically inverse associations for SON and similar but insignificant associations for DJF and MAM. Precipitation demonstrates significant associations with total PW at the annual level but does so only for DJF and JJA at the seasonal level. Little or no association, of any nature, between PW and precipitation is evident for MAM and SON.

Precipitable water characteristics by SC and season are presented in Table 3. Clear intersynoptic category contrasts in PW are apparent. Generally the highest PW values in any season are associated with synoptic categories that represent air masses originating to the south of the study area over the Mediterranean Sea (Fig. 3a). These are a consequence of a low zonal flow index attributable to a well-developed trough over France and the Iberian Peninsula and a blocking high originating over northeast Africa and the Arabian Peninsula that stretches northward over Turkey and the Black Sea region with concomitant strong southerly flows over southern Italy and Greece. Under such a synoptic setting air masses arriving over Greece have experienced a long ocean fetch and are thus very humid. In contrast SC with low PW are associated with quite a different synoptic-scale pressure configuration that results in airflows having a predominantly upwind land fetch. In the winter this situation is often associated with an extension of the Siberian high over eastern Europe, the consequence of which are strong cold dry flows of continental polar air over the Black Sea, Greece, and Italy (Fig. 3b). Although such air masses cross the Aegean Sea, the residence time of the air over this relatively warm water body is limited due to the high rates of airmass advection. Consequently the cool dry air has little time to sequester moisture from the warm sea surface. Therefore atmospheric moisture levels remain low in comparison to air masses originating over the Mediterranean Sea to the south of Greece.

A clear feature of the climatology of PW is its interannual variability, with some years showing strong positive (1978, 1989, 1994, 1999) and negative (1974, 1978, 1992) departures from the 28-yr mean (Fig. 4a). On a seasonal basis JJA possesses the greatest degree of variability followed by SON, DJF, and MAM in decreasing order of importance (Figs. 4b–e; Table 4). Consideration of the seasonal anomalies indicates that the large negative and positive annual anomalies in 1974 and 1999 are mostly associated with JJA moisture anomalies. Also in some years, such as 1997, strong negative departures in one season are compensated by strong positive anomalies in another season, the net effect being a damped anomaly at the annual level. Of the four seasons, DJF is notable for persistence of periods of positive and negative anomalies and is the only season that demonstrates any possible evidence of low-frequency variations in PW. Interestingly the persistent period of negative PW anomalies for the DJF 1988/89 to 1992/93 was followed by like anomalies in JJA from 1989 to 1992. However because of strong positive PW anomalies for SON (Fig. 4e), the period 1989 to 1992 does not appear anomalous at the annual level (Fig. 4a). Nevertheless the climatic effects of below-normal DJF and JJA PW levels for this period are manifest by a dry DJF and JJA (Fig. 5).

TABLE 4. Seasonal 500-hPa-level PW characteristics (mm) by synoptic category.

Season	Min	Max	Mean	Std dev
DJF	13.3	18.7	16.5	1.4
MAM	17.9	23.5	21.2	1.3
JJA	27.7	35.3	31.4	1.7
SON	23.1	28.7	25.9	1.6
Annual	22.5	25.7	23.8	0.62

Consideration of the association between the seasonal frequency of occurrence of synoptic categories and mean seasonal PW revealed that only some of the synoptic types appear to be important for explaining the interannual variation in seasonal PW (Table 5). For DJF higher PW values are associated with an increased (decreased) frequency of the synoptic type with the highest (lowest) PW (Tables 3 and 5). JJA also shows a similar relationship between the frequency of the wettest and driest synoptic categories and mean PW, as do MAM and SON.

b. *Precipitable water trends*

As well as interannual variability, a noteworthy characteristic is the apparent increase in PW values at the annual level (Fig. 4a) and for JJA and SON (Figs. 4d and 4e). To assess whether such trends are statistically significant annual and seasonal values of PW were regressed against time. Table 6 presents the rates of increase of PW in millimeters per decade for 1200 UTC and for the 850-, 700-, and 500-hPa isobaric layers, respectively. At the annual level significant increases in PW are apparent at all levels, with those between the surface and 700 hPa being the strongest. For all seasons there is a gradual increase in PW with the exception of MAM. However, trends are only significant for JJA and SON. The negligible decreases in PW for MAM most likely act to moderate the trends at the annual level.

Trends in PW by synoptic category (millimeters per

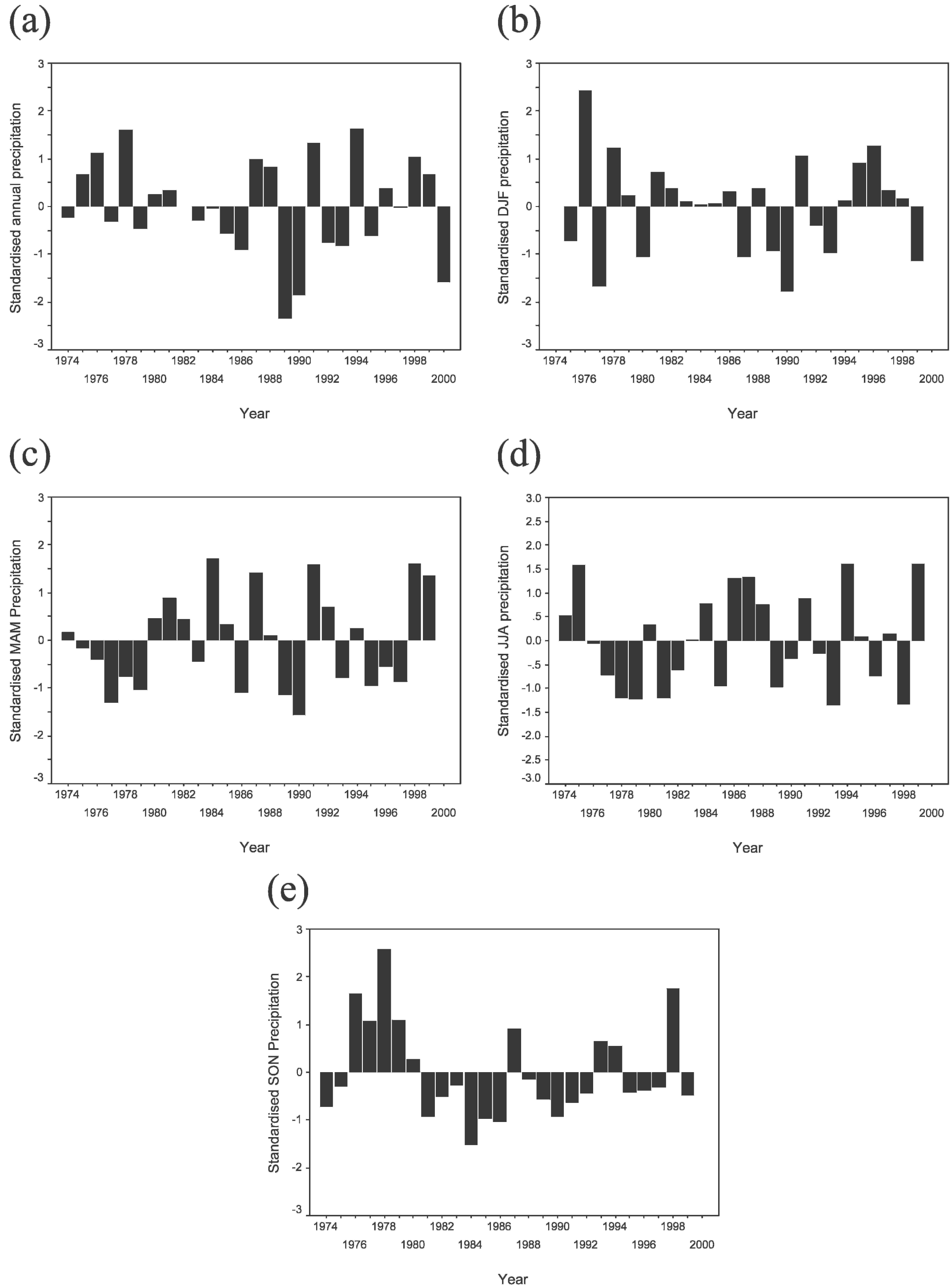

FIG. 5. Interannual variation of precipitation: (a) annual, (b) DJF, (c) MAM, (d) JJA, and (e) SON.

decade) are shown in Table 7. For DJF significant increases in PW exist for the moistest synoptic categories (SC 4 and 5). In contrast the driest synoptic category (SC 6), which is associated with air masses originating to the northeast of the study area, over eastern Europe (Fig. 3b), demonstrates decreases in PW. As noted previously, overall MAM demonstrates small but insignificant decreases in PW unlike the other seasons (Table 6). These would appear to be attributable to significant falls in PW for SC 1 and 3 that are compensated by

TABLE 5. Correlation between synoptic category frequency and mean PW by season, where *, **, and *** indicate significance at the 0.1, 0.05, and 0.01 levels, respectively.

	Synoptic category							
Season	1	2	3	4	5	6	7	8
DJF	−0.37*	0.31	−0.04	0.24	0.37*	−0.11	0.15	0.13
MAM	−0.19	−0.23	−0.33*	0.36*	0.48**	0.50**	0.29	0.01
JJA	0.33*	−0.27	0.65***	−0.56***				
SON	0.35*	0.08	0.24	−0.19	0.23	−0.43**	−0.06	−0.28

increases in PW for SC 5 and 6 (Table 7) associated with maritime air masses originating from the south over the Mediterranean Sea. For JJA three of the four synoptic categories possess increases in PW but only those for SC1 are significant. A weak pressure gradient over Greece in the early period of JJA, favoring the generation of sea breezes from the southwest, typifies this category. Increases in total PW for SON appear to be largely attributable to SC 1, 3, and 7 (Table 7), which are associated with air masses originating from the southwest and southeast over the Mediterranean Sea (Table 1) as a result of subtle changes in the location and intensity of an area of low pressure over the central Mediterranean west of Italy. While the decreases in PW for SON synoptic categories 4 and 8 are not significant, the northerly to easterly origin of the associated air masses strongly contrasts with that of SON categories 1 and 7 for which increases in PW have been noted.

Although the results presented in Table 7 are strongly suggestive of basic changes to the inherent PW properties of maritime and continental air masses over the study area, these results do not reveal whether changes in seasonal PW are occurring independently of changes in airmass frequency (Table 8). For example, the significant increase in PW for DJF could be due to a significant increase in the occurrence of one of the moist synoptic categories independent of basic changes in the intrinsic moisture properties of the associated air mass. Alternatively, increases in PW, without changes in synoptic category frequency, may also account for the observed trends. The latter would imply fundamental changes to an air mass' moisture properties.

TABLE 6. Seasonal and annual trend (mm decade^{-1}) in PW for three levels, where *, **, and *** indicate significance at the 0.1, 0.05, and 0.01 levels, respectively.

Season	850 hPa	700 hPa	500 hPa
DJF	0.11	0.09	0.01
MAM	−0.03	−0.17	−0.03
JJA	0.45**	0.69**	0.49**
SON	0.36*	0.69**	0.76*
Annual	0.23***	0.35***	0.27*

To assess the combined effects of changing synoptic category frequency (Table 8) and PW properties, the weighted contribution of each synoptic category to the mean seasonal PW amount was calculated for each year. The weighted contributions were then regressed against time so as to establish which of the synoptic categories demonstrate significant trends in terms of their contribution to seasonal PW levels (Table 9). Of the four seasons, only DJF and JJA possess synoptic categories with significant changes in their contribution to the mean level of PW. For DJF, the increasing importance of SC 1 (Table 9) for overall mean PW appears to be attributable to a significant increase in its frequency (Table 8) as opposed to increasing moisture levels (Table 7). This contrasts with SC 6 (the driest DJF category), as the declining importance of this synoptic type appears to be due to significant drying (Table 7), as no notable decreases in frequency exist (Table 8). SC 2 also displays a decreasing importance. In this case the changes are likely to be related to significant changes in both frequency and PW properties.

Near-significant trends in PW and frequency contribute to the growing importance of the moistest synoptic category for mean PW levels for JJA. Although significant trends are not apparent, JJA synoptic categories 1 and 4 display a diminished level of importance for overall JJA PW levels toward the end of the study period (Table 9). In the case of SC 1, this is obtained through a significant decrease in SC 1 frequency (Table 8) despite an increase in PW (Table 7). For JJA SC 4, the seemingly declining importance of this category is likely to be a result of a significant downturn in its frequency of occurrence (Table 8), as PW characteristics remain essentially unaltered over the study period (Table 7). For SON, SC 4 is the only category for which the magnitude of the trend in weighted contribution approaches that found in the other seasons, the sign of which may be related to a weak upward trend in the frequency of this category (Table 8) as the trend of PW is negative albeit insignificant (Table 7). SON SC 7 is of interest as a statistically significant fall in its frequency

TABLE 7. Trends in PW (mm decade^{-1}) by synoptic category, where *, **, and *** indicate significance at the 0.1, 0.05, and 0.01 levels, respectively.

	Synoptic category							
Season	1	2	3	4	5	6	7	8
DJF	0.2	−1.83**	0.05	1.5*	1.44***	−0.81**	1.44*	0.01
MAM	−1.24*	−0.64	−1.49*	0.92	0.96**	1.73***	0.65	0.49
JJA	1.15***	−0.58	0.65	−0.09				
SON	3.23**	−0.98	1.67**	−1.34	0.28	1.07	3.10***	−1.42**

of occurrence and an increasing level of PW conspires to produce a weak but insignificant downward trend in its weighted contribution (Table 9). At the overall level, MAM displays marginal but insignificant decreases in PW, undoubtedly a result of the negative weighted contribution for SC 2, 4, 5, and 7, which outweigh the positive contribution from SC 1, 3, 6, and 7 (Table 9). Noteworthy for MAM is the fact that the synoptic category with the highest PW levels (SC 4) is becoming less important in terms of its contribution to overall MAM PW levels. Consideration of the trends in PW and frequency in Tables 7 and 8 suggests that the less frequent occurrence of this SC may account for its demise as a contributor to PW levels for MAM.

4. Discussion and conclusions

An examination of a 28-yr record of monthly PW for southern Greece has revealed a clear seasonal cycle in PW as found for elsewhere (Bokoye et al. 2003; Chang et al. 1984; Chen 2004; Gueymard 1994; Lieberman et al. 2003; Nanjundiah and Srinivasan 1999; Picon et al. 2003; Okulov et al. 2002; Singh et al. 2000). This is somewhat a climatological expectation given the general relationship between atmospheric temperature and moisture as described by the Clausius–Clapeyron relationship (Rayner 2001). However, strong associations between surface temperature and total PW for the study area do not corroborate this, as for three of the seasons (DJF, MAM, and SON), there are anticorrelations between PW and surface temperature (Table 2). This may indicate that while tropospheric temperature exerts a general control on PW values for JJA, high PW levels in DJF, MAM, and SON may reflect high cloud cover such that surface radiation amounts and thus surface heating are reduced. This contention is somewhat supported by the association between PW and precipitation for DJF such that wet DJFs, and therefore a generally cloudy atmosphere, are linked with anomalously high PW levels (Table 2). For JJA, the positive association between PW and surface temperature may arise because high land surface temperatures associated with high pressure generate a high frequency of strong deep sea breezes that advect moist air from over the Mediterranean Sea across southern Greece (Melas et al. 1995). These increase humidity levels to a considerable depth within the atmosphere (Helmis et al. 1998; Melas et al. 1995, 1998). As vertical ascent is subdued due to the large-scale synoptic situation, the opportunity for cloud and hence precipitation formation is much reduced. Consequently through positive feedback, surface heating enhances the strength of the sea-breeze system and thus the atmospheric moisture flux over the study area (Prezerakos 1986; Thunis and Cuvlier 2000).

Precipitable water displays considerable variability at the annual and seasonal scales. While it is beyond the scope of this study to diagnose the mechanisms responsible for this variability, atmospheric circulation variations, as manifest by interannual variations in airmass frequency, as shown in this study, and storm tracks (Maheras et al. 2001) are likely candidates. Over the study area such variations are controlled by large-scale modes of variability such as the North Atlantic Oscillation (Mariotti et al. 2002; Ruprecht et al. 2002) with

TABLE 8. Trend (days decade^{-1}) in synoptic category frequency, where *, **, and *** indicate significance at the 0.1, 0.05, and 0.01 levels, respectively.

	Synoptic category							
Season	1	2	3	4	5	6	7	8
DJF	3.8*	−2.9***	−0.45	1.15	−2.3	−1.9	0.7	1.3
MAM	0.7	0.4	2.7*	−2.3	−0.5	0.3	−1.8	2.4
JJA	−4.1**	−0.8	0.5	−3.6**				
SON	0.34	1.1	−2.1	1.6	−2.3*	−3.0	−2.3**	0.4

TABLE 9. Trend in weighted contribution (% decade^{-1}) of synoptic category to mean seasonal total PW, where *, **, and *** indicate significant trends at the 0.1, 0.05, and 0.01 levels, respectively.

	Synoptic category							
Season	1	2	3	4	5	6	7	8
DJF	4.2**	−3.9***	0.3	1.6	−1.9	−3.1**	1.2	0.7
MAM	0.5	−2.6	2.1	−1.5	−2.0	0.7	−2.5**	1.7
JJA	−3.1	0.8	5.1**	−2.8				
SON	2.0	0.8	0.7	2.5	−1.8	−1.8	−1.2	0.1

remote forcing from ENSO also a possibility (Cohen et al. 2000).

Of chief interest in this study is the trend in PW over southern Greece. Significant upward trends in PW are evident at the annual scale, which may be attributed to significant increases in PW for JJA and SON. Although conservative in comparison, the annual trend matches that found for diverse regions such as North America and some parts of Europe (Ross and Elliott 2001), the western tropical Pacific (Gutzler 1992), China (Zhai and Eskridge 1997), and the global ocean (Wentz and Schabel 2000). At the annual level and for JJA, trends in PW are concomitant with upward trends in temperature over the study area, a response that might be expected with observed regional and global warming (Table 10). Conversely, despite strong trends in temperature, MAM possesses slight, although insignificant, decreases in PW. Furthermore SON, which demonstrates a significant fall in mean temperature, demonstrates rising PW levels (Table 10). Given this, it would appear that while atmospheric warming may directly account for fundamental changes to the moisture status of the JJA atmosphere over southern Greece, any warming-related effects on the other seasons are likely to be indirect and via, for example, changes in atmospheric circulation and thus atmospheric moisture transport.

A unique feature of this study is the disaggregation of seasonal PW trends according to a computer-assisted synoptic classification scheme and the consideration of the weighted contribution of individual synoptic types to overall seasonal PW levels. This has revealed that despite fundamental changes to the intrinsic PW properties for some synoptic categories, their significance for determining the overall trend in seasonal PW levels is tied to their frequency of occurrence. Consequently, the climatological effects of a moistening air mass may be offset by a declining frequency. Notwithstanding this, the strong trends in the PW status of some of the synoptic categories cannot be ignored. Generally the maritime air masses that cross the study area appear to be moistening while their continental counterparts appear to be drying. Trends in the frequency of these opposing air masses therefore holds implications for the future PW climatology and climate of the eastern Mediterranean as variations in moisture advection over Europe have been shown to play a substantial role in surface warming through the water vapor feedback effect (Otterman et al. 2002).

The fact that PW trends cannot be attributed solely to airmass warming points to the importance of other thermo-dynamical and hydrological factors for determining PW trends. Possibilities include modifications to surface evaporation rates due to changing Mediterranean sea surface temperatures in the case of maritime air masses (Bethoux et al. 1998; Casey and Cornillon 2001; Moron 2003; Rowell 2003; Schiano et al. 2005) or shifts in land surface hydrological processes (Koster and Suarez 2001; Pitman 2003; Wang et al. 2003; Zhao and Pitman 2002), which may affect the continental air masses that cross southern Greece. Alternatively, rates of moisture advection may have changed as a consequence of alterations to the intensity of the meridional circulation (Dunkeloh and Jacobeit 2003). Such contentions provide the basis for a future research agenda on

TABLE 10. Trends (+/−) in surface temperature (°C decade^{-1}) by synoptic category, where *, **, and *** indicate significance of the temperature trend at the 0.1, 0.05, and 0.01 levels, respectively. Arrows indicate whether a synoptic category possesses a statistically significant increase (↑) or decrease (↓) in PW (see Table 7).

Season	1	2	3	4	5	6	7	8
DJF	−0.01	−0.83↑	−0.22	−0.82↑	−0.5*↑	0.7↓	−1.2**↑	0.87***
MAM	2.75***↓	2.31***	3.4***↓	3.53***	3.32***↑	3.3***↑	2.4***	2.27***
JJA	1.7***↑	−0.33	0.58*	1.2***				
SON	−1.10↑	−2.65***	−2.04***↑	−2.63***	−1.49**	−1.61**	−2.61***↑	−2.99***↓

the PW climatology of southern Greece and the wider eastern Mediterranean region.

Acknowledgments. The authors thank both the Greek Meteorological Service and British Atmospheric Data Center (BADC) for kindly providing the radiosonde and surface climate data. The constructive comments provided by the anonymous reviewers have led to a marked improvement in the paper. These and the helpful guidance from the editor are gratefully acknowledged.

REFERENCES

Angell, J. K., W. P. Elliott, and M. E. Smith, 1984: Tropospheric humidity variations at Brownville, Texas and Great Falls, Montana, 1958–80. *J. Climate Appl. Meteor.,* **23,** 1286–1296.

Bethoux, J. P., B. Gentili, and D. Tailliez, 1998: Warming and freshwater budget change in the Mediterranean since the 1940s, their possible relation to the greenhouse effect. *Geophys. Res. Lett.,* **25,** 1023–1026.

Bokoye, A. I., A. Royer, N. T. O'Neill, P. Cliche, J. B. McArthur, P. M. Teillet, G. Fedosejevs, and J. M. Theriault, 2003: Multisensor analysis of integrated atmospheric water vapor over Canada and Alaska. *J. Geophys. Res.,* **108,** 4480, doi:10.1029/2002JD002721.

Bony, S., and J. P. Duvel, 1994: Influence of the vertical structure of the atmosphere on the seasonal-variation of precipitable water and greenhouse-effect. *J. Geophys. Res.,* **99** (D6), 12 963–12 980.

Casey, K. S., and P. Cornillon, 2001: Global and regional sea surface temperature trends. *J. Climate,* **14,** 3801–3818.

Chang, H. D., P. H. Hwang, T. T. Wilheit, A. T. C. Chang, D. H. Staelin, and P. W. Rosenkranz, 1984: Monthly distributions of precipitable water from the NIMBUS-7 SMMR DATA. *J. Geophys. Res.,* **89,** 5328–5334.

Chen, G., 2004: A 10-yr climatology of oceanic water vapor derived from the TOPEX Microwave Radiometer. *J. Climate,* **17,** 2541–2557.

Chen, T. C., and R. Y. Tzeng, 1990: Global-scale intraseasonal and annual variation of divergent water-vapor flux. *Meteor. Atmos. Phys.,* **44,** 133–151.

——, J. Pfaendtner, J. M. Chen, and C. K. Wikle, 1996a: Variability of the global precipitable water with a timescale of 90–150 days. *J. Geophys. Res.,* **101** (D5), 9323–9332.

——, M. C. Yen, J. Pfaendtner, and Y. C. Sud, 1996b: Annual variation of the global precipitable water and its maintenance: Observation and climate-simulation. *Tellus,* **48A,** 1–16.

Chrysoulakis, N., and C. Cartalis, 2002: Improving the estimation of land surface temperature for the region of Greece: Adjustment of a split window algorithm to account for the distribution of precipitable water. *Int. J. Remote Sens.,* **23,** 871–880.

Cohen, J. L., D. A. Salstein, and R. D. Rosen, 2000: Interannual variability in the meridional transport of water vapor. *J. Hydrometeor.,* **1,** 547–553.

Dunkeloh, A., and J. Jacobeit, 2003: Circulation dynamics of Mediterranean precipitation variability 1948–98. *Int. J. Climatol.,* **23,** 1843–1866.

Elliott, W. P., and D. J. Gaffen, 1991: On the utility of radiosonde humidity archives for climate studies. *Bull. Amer. Meteor. Soc.,* **72,** 1507–1519.

——, and J. K. Angell, 1997: Variations of cloudiness, precipitable water, and relative humidity over the United States: 1973–1993. *Geophys. Res. Lett.,* **24,** 41–44.

Forster, P. M. D., and K. P. Shine, 2002: Assessing the climate impact of trends in stratospheric water vapor. *Geophys. Res. Lett.,* **29,** 1086, doi:10.1029/2001GL013909.

——, and M. Collins, 2004: Quantifying the water vapour feedback associated with post-Pinatubo global cooling. *Climate Dyn.,* **23,** 207–214.

Free, M., and Coauthors, 2002: Creating climate reference datasets: Cards workshop on adjusting radiosonde temperature data for climate monitoring. *Bull. Amer. Meteor. Soc.,* **83,** 891–899.

——, J. K. Angell, I. Durre, J. Lanzante, T. C. Peterson, and D. J. Seidel, 2004: Using first differences to reduce inhomogeneity in radiosonde temperature datasets. *J. Climate,* **17,** 4171–4179.

Gaffen, D. J., M. A. Sargent, R. E. Haberman, and J. R. Lazante, 2000: Sensitivity of tropospheric and stratospheric temperature trends to radiosonde data quality. *J. Climate,* **13,** 1776–1796.

Gueymard, C., 1994: Analysis of monthly average atmospheric precipitable water and turbidity in Canada and northern United-States. *Sol. Energy,* **53,** 57–71.

Gutman, S. I., S. R. Sahm, S. G. Benjamin, B. E. Schwartz, K. L. Holub, J. Q. Stewart, and T. L. Smith, 2004: Rapid retrieval and assimilation of ground based GPS precipitable water observations at the NOAA forecast systems laboratory: Impact on weather forecasts. *J. Meteor. Soc. Japan,* **82,** 351–360.

Gutzler, D., 1992: Climatic variability of temperature and humidity over the tropical western Pacific. *Geophys. Res. Lett.,* **19,** 1839–1879.

Helmis, C. G., K. H. Papadopoulos, J. A. Kalogiros, and A. T. Soilemes, 1998: Influence of background flow on evolution of Saronic gulf sea breeze. *Atmos. Environ.,* **29,** 3689–3701.

Hense, A., P. Krahe, and H. Flohn, 1988: Recent fluctuations of tropospheric temperature and humidity over the western Pacific. *Meteor. Atmos. Phys.,* **38,** 215–227.

Hollander, M., and D. A. Wolfe, 1973: *Nonparametric Statistical Inference.* John Wiley & Sons, 503 pp.

Kane, R. P., 1996: Interannual variability of precipitable water. *Ann. Geophys. Atmos. Hydrosph. Space Sci.,* **14,** 464–467.

Kassomenos, P., 2003a: Anatomy of the synoptic conditions occurring over southern Greece during the second half of the 20th century. Part I. DJF and JJA. *Theor. Appl. Climatol.,* **75,** 65–77.

——, 2003b: Anatomy of the synoptic conditions occurring over southern Greece during the second half of the 20th century. Part II. SON and MAM. *Theor. Appl. Climatol.,* **75,** 79–92.

Koster, R. D., and M. J. Suarez, 2001: Soil moisture memory in climate models. *J. Hydrometeor.,* **2,** 558–570.

Lanzante, J. R., 1996: Resistant, robust and non-parametric techniques for the analysis of climate data: Theory and examples, including applications to historical radiosonde station data. *Int. J. Climatol.,* **16,** 1197–1226.

——, S. A. Klein, and D. J. Seidel, 2003a: Temporal homogenization of monthly radiosonde temperature data. Part II: Methodology. *J. Climate,* **16,** 224–240.

——, ——, and ——, 2003b: Temporal homogenization of monthly radiosonde temperature data. Part II: Trends, sensitivities, and MSU comparison. *J. Climate,* **16,** 241–262.

Li, Z. L., L. Jia, Z. B. Su, Z. M. Wan, and R. H. Zhang, 2003: A new approach for retrieving precipitable water from ATSR2 split-window channel data over land area. *Int. J. Remote Sens.,* **24,** 5095–5117.

Lieberman, R. S., D. A. Ortland, and E. S. Yarosh, 2003: Climatology and interannual variability of diurnal water vapor heating. *J. Geophys. Res.*, **108,** 4123, doi:10.1029/2002JD002308.

Liu, J., and R. E. Stewart, 2003: Water vapor fluxes over the Saskatchewan River basin. *J. Hydrometeor.,* **4,** 944–959.

Long, M., D. Entekhabi, and S. E. Nicholson, 2000: Interannual variability in rainfall, water vapor flux, and vertical motion over West Africa. *J. Climate,* **13,** 3827–3841.

Maheras, P., H. A. Flocas, I. Patrikas, and C. Anagnostopoulou, 2001: A 40 year objective climatology of surface cyclones in the Mediterranean region: Spatial and temporal distribution. *Int. J. Climatol.,* **21,** 109–130.

Mariotti, A., M. V. Struglia, N. Zeng, and K.-M. Lau, 2002: The hydrological cycle in the Mediterranean region and implications for the water budget of the Mediterranean Sea. *J. Climate,* **15,** 1674–1690.

Marsden, D., and F. P. J. Valero, 2004: Observation of water vapor greenhouse absorption over the Gulf of Mexico using aircraft and satellite data. *J. Atmos. Sci.,* **61,** 745–753.

McGregor, G. R., and S. Nieuwolt, 1998: *Tropical Climatology: An Introduction to the Climate of the Low Latitudes*. J. Wiley and Sons, 339 pp.

——, C. A. T. Ferro, and D. B. Stephenson, 2005: Projected changes in extreme weather and climate events in Europe. *Extreme Weather Events and Public Health Responses,* W. Kirch, B. Menne, and R. Bertollini, Eds., Springer, 290 pp.

Melas, B., I. C. Ziomas, and C. S. Zerefos, 1995: Boundary layer dynamics in an urban coastal environment under sea breeze conditions. *Atmos. Environ.,* **29,** 3605–3617.

——, ——, O. Klemm, and C. S. Zerefos, 1998: Anatomy of the sea-breeze circulation in Athens area under weak large-scale ambient winds. *Atmos. Environ.,* **32,** 2223–2237.

Moron, V., 2003: Long-term variability of the Mediterranean Sea surface temperature (1856–2000). *Compt. Rend. Geosci.,* **335,** 721–727.

Myers, D. S., and D. E. Waliser, 2003: Three-dimensional water vapor and cloud variations associated with the Madden–Julian oscillation during Northern Hemisphere DJF. *J. Climate,* **16,** 929–950.

Nanjundiah, R. S., and J. Srinivasan, 1999: Anomalies of precipitable water vapour and vertical stability during El Nino. *Geophys. Res. Lett.,* **26,** 95–98.

Ohmura, A., and M. Wild, 2002: Is the hydrological cycle accelerating? *Science,* **298,** 1345–1346.

Okulov, O., H. Ohvril, and R. Kivi, 2002: Atmospheric precipitable water in Estonia, 1990–2001. *Bor. Environ. Res.,* **7,** 291–300.

Otterman, J., J. Angell, R. Atlas, D. Bungato, S. Schubert, D. Starr, J. Susskind, and M. L. C. Wu, 2002: Advection from the North Atlantic as the forcing of DJF greenhouse effect over Europe. *Geophys. Res. Lett.*, **29,** 1241, doi:10.1029/2001GL014187.

Parry, M. L., Ed., 2000: Assessment of the potential effects and adaptations for climate change in Europe: The Europe ACACIA Project. Jackson Environment Institute, University of East Anglia, Norwich, United Kingdom, 320 pp.

Peterson, T. C., and Coauthors, 1998: Homogeneity adjustments of in situ atmospheric climate data: A review. *Int. J. Climatol.,* **18,** 1493–1517.

Peixoto, J. H., and A. H. Ort, 1992: *Physics of Climate*. American Institute of Physics, 520 pp.

Phillips, I. D., and G. R. McGregor, 2001: Western European water vapor flux–southwest England rainfall associations. *J. Hydrometeor.,* **2,** 505–524.

Picon, L., R. Roca, S. Serrar, J. L. Monge, and M. Desbois, 2003: A new METEOSAT "water vapor" archive for climate studies. *J. Geophys. Res.*, **108,** 4301, doi:10.1029/2002JD002640.

Pitman, A. J., 2003: The evolution of, and revolution in, land surface schemes designed for climate models. *Int. J. Climatol.,* **23,** 479–510.

Prezerakos, N., 1986: Characteristics of the sea breezes in Attica. *Bound.-Layer Meteor.,* **36,** 245–266.

Rayner, J. N., 2001: *Dynamic Climatology*. Blackwell, 279 pp.

Ross, R. J., and W. P. Elliott, 2001: Radiosonde-based Northern Hemisphere tropospheric water vapor trends. *J. Climate,* **14,** 1602–1612.

Rowell, D. P., 2003: The impact of Mediterranean SSTs on the Sahelian rainfall season. *J. Climate,* **16,** 849–862.

Ruprecht, E., S. S. Schroder, and S. Ubl, 2002: On the relation between NAO and water vapour transport towards Europe. *Meteor. Z.,* **11,** 395–401.

Sajith, V., K. R. Santosh, and H. S. R. Mohan, 2003: Intraseasonal oscillation of total precipitable water over North Indian Ocean and its application in the diagnostic study of coastal rainfall. *Geophys. Res. Lett.,* **30,** 2054, doi:10.1029/2003GL017635.

Schiano, M. E., S. Sparnocchia, C. Cappa, and R. Bozzano, 2005: An analysis of the climate variability over the Mediterranean Sea by means of the surface water vapour density. *Int. J. Climatol.,* **25,** 1731–1748.

Simmonds, I., D. H. Bi, and P. Hope, 1999: Atmospheric water vapor flux and its association with rainfall over China in summer. *J. Climate,* **12,** 1353–1367.

Singh, R. P., N. C. Mishra, A. Verma, and J. Ramaprasad, 2000: Total precipitable water over the Arabian Ocean and the Bay of Bengal using SSM/I data. *Int. J. Remote Sens.,* **21,** 2497–2503.

Smirnov, V. V., and G. W. K. Moore, 2001: Short-term and seasonal variability of the atmospheric water vapor transport through the Mackenzie River basin. *J. Hydrometeor.,* **2,** 441–452.

Thunis, P., and C. Cuvlier, 2000: Impact of biogenic emissions on ozone formation in the Mediterranean area—A BEMA modeling study. *Atmos. Environ.,* **34,** 467–481.

Trenberth, K. E., 2004: Manifestations of global climate change on accelerating the hydrological cycle: Prospects for increases in extremes. *Proc. Second Int. CAHMDA Workshop on the Terrestrial Water Cycle: Modelling and Data Assimilation across Catchment Scales*, Princeton, NJ, 37–39.

Vladimir, V., S. Smirnov, and G. W. K. Moore, 2002: Short-term and seasonal variability of the atmospheric water vapor transport through the Mackenzie River basin. *J. Hydrometeor.,* **2,** 441–452.

Wang, H., A. J. Pitman, M. Zhao, and R. Leemans, 2003: The impact of land-cover modification on the June meteorology of China since 1700, simulated using a regional climate model. *Int. J. Climatol.,* **23,** 511–527.

Wentz, F. J., and M. Schabel, 2000: Precise climate monitoring using complementary satellite data sets. *Nature,* **403,** 414–416.

Zhai, P., and R. E. Eskridge, 1996: Analyses of inhomogeneities in radiosonde temperature and humidity time series. *J. Climate,* **9,** 884–894.

——, and ——, 1997: Atmospheric water vapor over China. *J. Climate,* **10,** 2643–2652.

Zhao, M., and A. J. Pitman, 2002: The regional scale impact of land cover change simulated with a climate model. *Int. J. Climatol.,* **22,** 271–290.

Zveryaev, I. I., and P. S. Chu, 2003: Recent climate changes in precipitable water in the global tropics as revealed in National Centers for Environmental Prediction/National Center for Atmospheric Research reanalysis. *J. Geophys. Res.,* **108,** 4311, doi:10.1029/2002JD002476.